DOI 10.5012/bkcs.2011.32.8.2560

Adsorption Behavior of Environmental Hormone Bisphenol A onto Mesoporous Silicon Dioxide

Xianghong Fan,* Bing Tu, Hongmei Ma, and Xuefen Wang

*Renmin Hospital of Wuhan University, Wuhan 430060, China. *E-mail address: fxhwhu@163.com*
Received May 7, 2011, Accepted June 14, 2011

Mesoporous silicon dioxide (*meso*-SiO_2) was prepared using cetyltrimethylammonium bromide as the structure-directing reagent and tetraethyl orthosicate as the silicon source. The influence of pH value on the adsorption behavior of bisphenol A (BPA) was investigated. The adsorption capacity of BPA onto *meso*-SiO_2 increases slightly with pH value from 2 to 6, and then gradually decreases as further improving pH value. The effect of temperature was also studied, and the adsorption capacity of BPA gradually declines with increasing temperature. The adsorption kinetics and thermodynamics of BPA were examined. It is found that the adsorption of BPA onto *meso*-SiO_2 is in good agreement with Langmuir adsorption model. The rate constant of adsorption is 5.17×10^{-3} g mg^{-1} min^{-1}, and the maximum adsorption capacity is as high as 353.4 mg g^{-1} at 20 °C.

Key Words: Bisphenol A, Endocrine disrupting compound, Adsorption, Mesoporous silica

Introduction

Bisphenol A (4,4'-isopropylidenediphenol, BPA) has been widely used in the plastic industry as a monomer to produce epoxy resins and polycarbonate. BPA is ubiquitous in our life since it can be released into environment from numerous ways such as bottles, packaging, landfill leachates and plastics plants.[1-3] In the Unite states, the annual production capacity of BPA is about 865 000 tons.[4] Moreover, BPA was non-biodegradable and highly resistant to chemical degradation, so that the concentration of BPA in the environmental is frequently high. Researches have shown that BPA can mimic and influence hormonal activities *via* disrupting growth, development and reproduction.[5,6] Thus, BPA has been identified as an important endocrine disrupting compound (EDC). In addition, BPA was found to possibly cause caner, and an association between BPA and breast cancer has been discovered.[7,8] Therefore, it is quite important to study the adsorption behavior of BPA and to develop highly-efficient adsorbent for BPA.

Up-to-now, the adsorption behavior of BPA has been extensively studied, and various materials have been reported, including cross-linked β-cyclodextrin polymer with maximum adsorption capacity (Q_m) of 84 mg g^{-1},[9] chitosan-bearing β-cyclodextrin with Q_m of 85 mg g^{-1},[10] esterified carboxyl cotton with of Q_m 87.7 mg g^{-1},[11] alpha-ketoglutaric acid-modified chitosan resins with Q_m of 60.7 mg g^{-1},[12] and organic-inorganic hybrid mesoporous silica with Q_m of 351 mg g^{-1}.[13] In addition, other materials such as mineral,[14] sludge,[15] and activated carbon[16,17] were also reported as adsorbent for BPA.

Mesoporous material is a kind of porous materials with regular and tunable pore from 2 to 50 nm. Since its discovery,[18] the interest in this field has expanded all over the world.[19] With the properties such as highly uniform channels, large surface area, narrow pore-size distribution and tunable pore sizes over a wide range, mesoporous materials have attracted considerable attention and obtained wide applications.[20,21] The main objective of this work is to examine the adsorption behavior of BPA on mesoporous silicon oxide (*meso*-SiO_2), and then to develop a highly-efficient adsorbent for BPA. The *meso*-SiO_2 was synthesized using cationic surfactant as the structure-directing template. After that, the adsorption kinetics and thermodynamics of BPA were investigated in great detail. The maximum adsorption capacity is 353.4 mg g^{-1}, suggesting that *meso*-SiO_2 is an excellent adsorbent for BPA.

Experimental Section

Materials. Bisphenol A (BPA, 97%) was purchased from Acros (New Jersey, USA), and dissolved into ethanol to prepare 1 g L^{-1} stock soluiton. Cetyltrimethylammonium bromide (CTAB, purity > 99.0%), tetraethyl orthosicate (TEOS, analytical grade, SiO_2 purity > 28.4%), NaCl, HCl and NaOH were purchased from the Siompharm Group Chemical Reagent Co. Ltd., China. The used water is redistilled. All the chemicals were used directly without purification.

Instruments. The ultraviolet-visible (UV-vis) spectrogram was conducted on an UV-2550 spectrophotometer (SHIMADZU, Japan). The pH value of solution was measured using a Model PHS-3C pH meter (Shanghai Precision & Scientific Instrument Co. LTD, China). Scanning electron microscopy (SEM) was performed with a Quanta 200 microscope (FEI Company, Netherlands). Infrared spectrogram was measured using a VERTEX 70 Fourier Transform Infrared Spectrometer (Bruker, Germany).

Synthesis of *meso*-SiO_2. *meso*-SiO_2 was synthesized as the reported method[22] using CTAB as the template. In 90.0

mL water, 1.82 g CTAB and 0.05 g NaOH was added into, and then stirred at 25 °C to form a clear solution. After that, 11.35 mL TEOS was added into the solution under stirring to give a gel mixture. After 30 min of stirring at 25 °C, the mixture was sealed and then heated at 70 °C for 24 h under static conditions. The resulting solid precipitate was recovered by filtration, washed with re-distilled water and then dried at 80 °C for 12 h. Finally, the dried solid precipitate was calcined at 550 °C for 8 h to remove CTAB and form mesopores.

Batch Adsorption. All batch adsorption studies were conducted in the lined capped glass bottles containing 100.0 mL solution. All batch reactors were placed on a reciprocating shaker (SHZ-82 A, Changzhou Guohua Electric Appliance Company, China) at 150 rpm and under controlled temperature of 20 °C. Each experiment was carried out in triplicate and the average value was used.

Results and Discussion

Detection of BPA Concentration. In order to achieve the concentration of BPA solution, the absorption behavior of BPA was studied. Figure 1 shows the UV-vis spectrograms of BPA in 0.01 M NaCl solution with pH of 6. During the wavelength scan from 250 to 350 nm, an absorption peak was observed at 276 nm, which is the B band and attributed to the π-π* electronic transition of aromatic ring. When we change the concentration of BPA, it is found that the absorption peak alters correspondingly. So the absorbance (A) at 276 nm can be used as the analytical signal for BPA. As shown in Figure 2, the value of A is proportional to the concentration of BPA over the range from 0 to 80 mg L^{-1} (C), and obeys the following equation: A = 0.01325 C. The correlation coefficient (R) is 0.9986, indicating excellent linearity.

Characterization of *meso*-SiO_2. Figure 3 depicts the infrared (IR) spectrograms of SiO_2 before (a) and after calcination (b). From the comparison, it is apparent that there are three absorption peaks at 2915 cm^{-1}, 2842 cm^{-1} and 1479 cm^{-1} before calcination. The peaks at 2915 cm^{-1} and 2842 cm^{-1} are caused by the stretching vibration of -CH_3 and -CH_2 in the CTAB molecule. While the peak of 1479 cm^{-1} is due to the flexural vibration of -CH_2. After calcination at 550 °C for 8 h, these three peaks vanished, suggesting that CTAB was removed from SiO_2.

The morphology and grain size of prepared *meso*-SiO_2 were characterized using SEM. From the SEM image in Figure 4, it is clear that the synthesized *meso*-SiO_2 is com-

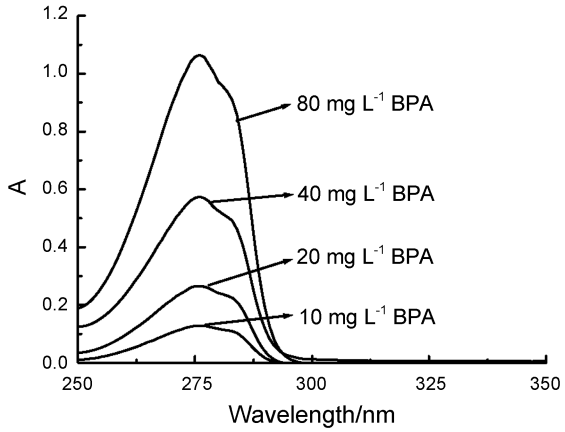

Figure 1. UV-vis spectrograms of BPA in 0.01 M NaCl solution at pH of 6.

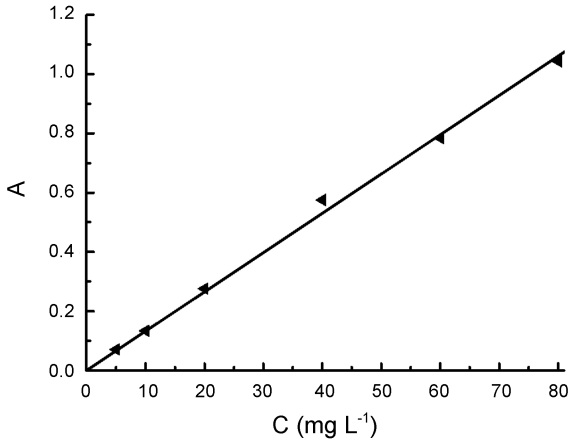

Figure 2. Calibration curve for BPA.

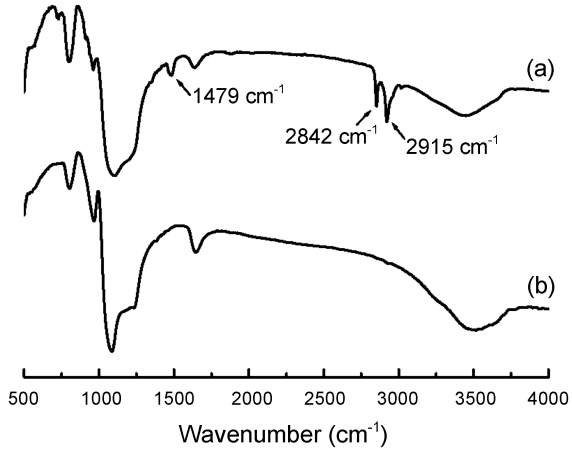

Figure 3. FT-IR spectrograms of SiO_2 before (a) and after calcination (b).

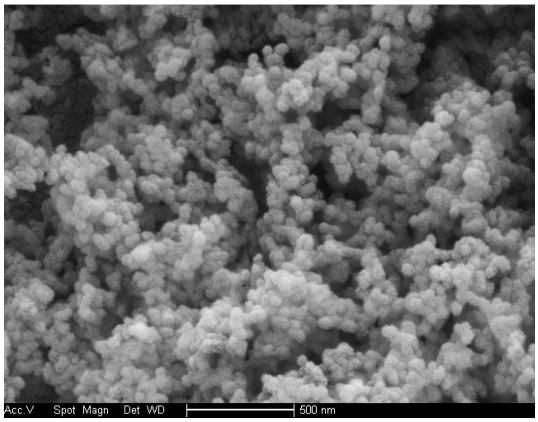

Figure 4. SEM image of *meso*-SiO_2.

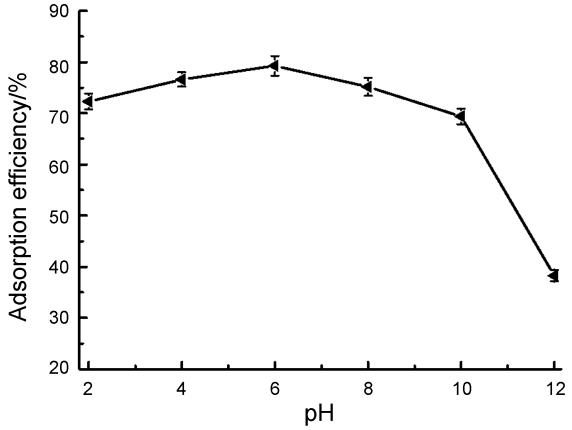

Figure 5. Effect of pH value on the adsorption of BPA onto *meso*-SiO_2. BPA concentration is 40.0 mg L^{-1}, and its loading is 0.5 g L^{-1}. The error bars represent the standard deviation of triplicate measurements.

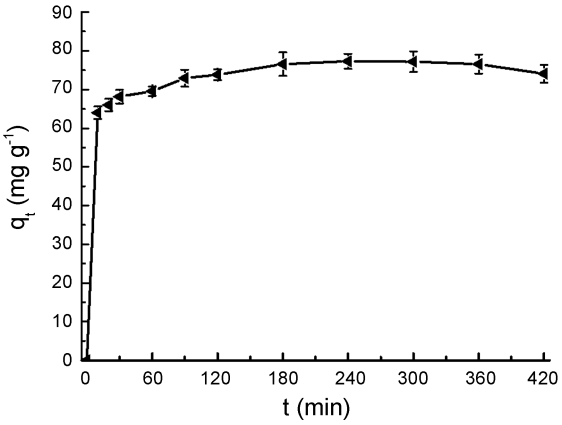

Figure 6. Kinetic curve of BPA. Other condition as in Figure 5.

posed of well-dispersed spherical nanoparticles, and the particle size is about 40 nm.

Influence of pH. The impact of pH value on the adsorption behavior of BPA was examined. In 100.0 mL of 0.01 M NaCl solution containing 40.0 mg L^{-1} BPA, the pH value was adjusted to different values using 0.1 M NaOH and HCl. After that, 50.0 mg *meso*-SiO_2 was added into the solution, and then shaked at 150 rpm for 30 min. Finally, all the suspensions were filtered using 0.45 mm membrane, and then analyzed for BPA using UV-vis spectrophotometer. The adsorption efficiency was then calculated from equation (1).

$$\text{adsorption efficiency} = \frac{(C_i - C_t)}{C_i} \quad (1)$$

The C_i and C_t depicts the concentration before and after adsorption (mg L^{-1}). As shown in Figure 5, the adsorption efficiency of BPA onto *meso*-SiO_2 increases slightly when pH value enhances from 2 to 6. With further increasing the pH value to 10, the adsorption efficiency of BPA shows slight decline. This phenomenon reveals that the influence of pH value is not severe over the range from 2 to 10. However, the adsorption ability of *meso*-SiO_2 toward BPA gradually decreases when pH increasing from 10 to 12, suggesting that high pH value is unbeneficial for the adsorption of BPA. In order to get higher adsorption efficiency, the suitable pH value was controlled at 6.

Adsorption Kinetics. Adsorption kinetics was conducted to study the adsorption rate of BPA and to obtain the equilibrium time for adsorption isotherm. The experiments were performed at pH 6, and the initial BPA concentration is 40.0 mg L^{-1}. In each test, 50.0 mg *meso*-SiO_2 was used, resulting in an adsorbent loading of 0.5 g L^{-1}. After different adsorption time, the suspension was filtered, and the content of BPA in solution was detected. The adsorption capacity of BPA at any time (q_t, mg g^{-1}) was determined by equation (2).

$$q_t = \frac{(C_i - C_t)V}{M} \quad (2)$$

M is the dry mass of adsorbent (g), V is volume of the solution (L). The adsorption kinetic curve of BPA on *meso*-SiO_2 is shown in Figure 6. When the adsorption time extends from 0 to 10 min, the q_t sharply increases from 0 to 64%, indicative of a rapid adsorption process. After 10 min, the q_t increases slightly with adsorption time, and reaches maximum at 240 min. According to the reported results[23] and Figure 6, it is apparent that the adsorption of BPA on *meso*-SiO_2 contains two essential steps: rapid adsorption and slow adsorption. The rapid adsorption mainly occurs at the relatively weak adsorption site on the external and/or in the porous channel of *meso*-SiO_2. While the slow adsorption is caused by a diffusion-controlled step in which the adsorption takes place on the intraparticle site of *meso*-SiO_2. However, the q_t decreases very slightly as the adsorption time increases from 240 min to 420 min, maybe due to the weak desorption.

To further analyze the adsorption rate of BPA, a pseudo-second-order rate equation was used to simulate the kinetic adsorption:[24]

$$\frac{dq_e}{d_t} = k_2(q_e - q_t)^2 \quad (3)$$

where k_2 (g mg^{-1} min^{-1}) is the rate constant of pseudo-second-order adsorption, q_e (mg g^{-1}) and q_t (mg g^{-1}) are the adsorption capacity at equilibrium and at time of t. Integrating Equation (3) for boundary conditions $t = 0$ to $t = t$ as well as $q_t = 0$ to $q_t = q_t$ gives the equation (4).

$$\frac{t}{q_t} = \frac{1}{k_2 q_e^2} + \frac{t}{q_e} \quad (4)$$

So the plot of t/q_t versus t is a straight line, and the value of q_e and k_2 can be easily achieved from the slope and interception. As to BPA on *meso*-SiO_2, the curve of t/q_t to t is a line, which is shown in Figure 7. The value of slope and interception is 0.0131 and 0.03318, respectively. As a result, the q_e and k_2 was calculated to 76.34 mg g^{-1} and 5.17×10^{-3} g mg^{-1} min^{-1}. In addition, the value of R is equal to 0.9951 and very close to the theoretical value of 1. Undoubtedly, the kinetic adsorption of BPA on *meso*-SiO_2 can be well described by a pseudo-order rate equation.

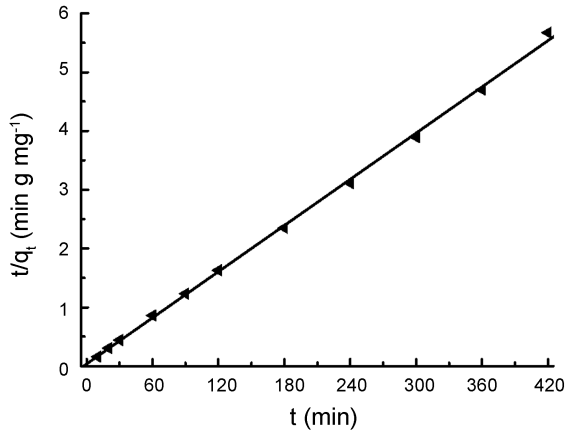

Figure 7. Plot of t/q_t versus t for adsorption of BPA onto *meso*-SiO_2. Other condition as in Figure 5.

Adsorption Thermodynamics. From the adsorption kinetic curve of BPA, the equilibrium adsorption time was fixed to 240 min for the rest of batch experiments to make sure that the equilibrium was achieved. The influences of initial concentration of BPA and the temperature on the equilibrium adsorption of BPA were studied for obtaining the adsorption isotherms. Adsorption isotherm experiments were measured at pH 6.0 and the adsorbent loading of 0.5 g L^{-1}. After 240 min of equilibrium, the suspension was filtered, and the concentration of BPA in the filtrate was analyzed. The equilibrium adsorption capacity of BPA onto *meso*-SiO_2 (q_e, mg g^{-1}) was defined by equation (5).

$$q_e = \frac{(C_i - C_e)V}{M} \tag{5}$$

Figure 8 illustrates the effect of initial concentration of BPA on the equilibrium adsorption capacity. At different temperatures, the equilibrium adsorption capacity of BPA onto *meso*-SiO_2 increases linearly with its initial concentration from 0 to 150 mg L^{-1}. With further improving the initial concentration to 175 mg L^{-1}, the enhancement of equilibrium adsorption capacity decreases, and the line becomes curved.

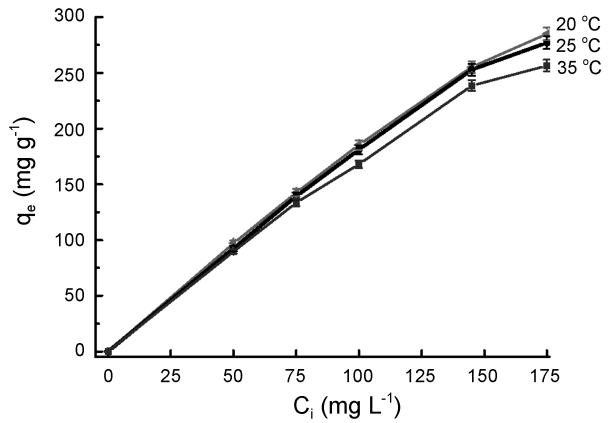

Figure 8. Influence of BPA concentration and temperature on its equilibrium adsorption capacity. Other condition as in Figure 5.

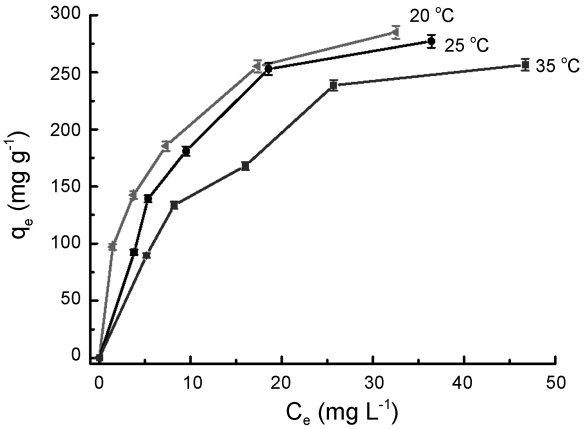

Figure 9. Adsorption isotherms of BPA onto *meso*-SiO_2 at 20 °C, 25 °C and 35 °C. Other condition as in Figure 5.

Table 1. Parameters of Langmuir adsorption of BPA onto *meso*-SiO_2 at different temperatures

	Q_m (mg g^{-1})	b (L mg^{-1})	R
20 °C	353.4	0.1586	0.9995
25 °C	349.7	0.1117	0.9962
35 °C	334.5	0.0811	0.9837

Figure 9 denotes the relationship between q_e and C_e of BPA. It is also fount that the value of q_e remarkably increases at first, and then increases slightly. The slight enhancement is possibly owing to the adsorption saturation. Additionally, the equilibrium adsorption capacity of BPA onto *meso*-SiO_2 gradually decreases with improving temperature, suggesting that the adsorption of BPA on *meso*-SiO_2 is an exothermic reaction.

Until now, there are several adsorption models such as Henry model, Freundlich model, Langmuir model and BET model. Among these models, Langmuir adsorption is very common and described by the equation (6):[25]

$$\frac{C_e}{q_e} = \frac{C_e}{Q_m} + \frac{1}{Q_m b} \tag{6}$$

where Q_m (mg g^{-1}) is the maximum adsorption capacity, b is the isotherm constant. Clearly, the plot of C_e/q_e versus C_e is a line for Langmuir adsorption, and the value of Q_m and b can be easily calculated from the slope and interception. Herein, we found that C_e/q_e changes linearly with C_e at all tested temperature, and the value of R is higher than 0.99. Without a doubt, the adsorption of BPA onto *meso*-SiO_2 can be well described using Langmuir equation. Table 1 gives the value of Q_m and b that calculated from the plot of C_e/q_e to C_e. The maximum adsorption capacity is as high as 353.4 mg g^{-1}, revealing that *meso*-SiO_2 is a highly-efficient adsorbent for BPA. As explained, the maximum adsorption capacity also decreases with increasing temperature.

Conclusions

A highly-efficient and environment-friendly adsorbent

was prepared for environmental hormone BPA. Using cationic surfactant as the template molecule, *meso*-SiO_2 was successfully synthesized. The adsorption behavior of BPA onto *meso*-SiO_2 obeys the Langmuir model, and the maximum adsorption capacity is as large as 353.4 mg g^{-1}. The adsorption of BPA on *meso*-SiO_2 is an exothermic reaction, and the adsorption efficiency decreases with increasing temperature.

References

1. Kolpin, D. W.; Furlong, E. T.; Meyer, M. T.; Thurman, E. M.; Zaugg, S. D.; Barber, L. B.; Buxton, H. T. *Environ. Sci. Technol.* **2002**, *36*, 1202.
2. Jin, X. L.; Jiang, G. B.; Huang, G. L.; Liu, J. F.; Zhou, Q. F. *Chemosphere* **2004**, *56*, 1113.
3. Torres, R. A.; Pétrier, C.; Combet, E.; Moulet, F.; Pulgarin, C. *Environ. Sci. Technol.* **2007**, *41*, 297.
4. Terasaki, M.; Shiraishi, F.; Nishikawa, T.; Edmonds, J. S.; Morita, M.; Makino, M. *Environ. Sci. Technol.* **2005**, *39*, 3703.
5. Jobling, S.; Nolan, M.; Tyler, C. R.; Brighty, G.; Sumpter, J. P. *Environ. Sci. Technol.* **1998**, *32*, 2498.
6. Kang, J. H.; Kondo, F.; Katayama, Y. *Toxicology* **2006**, *226*, 79.
7. Skakkebaek, N. E.; Meyts, E. R.; Jorgensen, N.; Carlsen, E.; Petersen, P. M.; Giwercman, A.; Andersen, A. G.; Jensen, T. K.; Andersson, A. M.; Müller, J. *APMIS* **1998**, *106*, 3.
8. Monica, M. T.; Markey, C. M.; Wadia, P. R.; Luque, E. H.; Rubin, B. S.; Sonnenschein, C.; Soto, A. M. *Endocrinology* **2005**, *146*, 4138.
9. Kitaoka, M.; Hayashi, K. *J. Incl. Phenom. Macrocycl. Chem.* **2002**, *44*, 429.
10. Aoki, N.; Arai, R.; Hattori, K. *J. Incl. Phenom. Macrocycl. Chem.* **2004**, *50*, 115.
11. Gong, R.; Liang, J.; Chen, J.; Huang, F. *Int. J. Environ. Sci. Technol.* **2009**, *6*, 539.
12. Gong, R. M.; Jiang, Y.; Cai, W. K.; Zhang, K.; Yuan, B.; Jiang, J. H. *Desalination* **2010**, *258*, 54.
13. Kim, Y. H.; Lee, B.; Choo, K. H.; Choi, S. *J. Microporous Mesoporous Mat.* **2011**, *138*, 184.
14. Shareef, A.; Angove, M. J.; Wells, J. D.; Johnson, B. B. *J. Colloid Interface Sci.* **2006**, *297*, 62.
15. Zhao, J. M.; Li, Y. M.; Zhang, C. J.; Zeng, Q. L.; Zhou, Q. *J. Hazard. Mate.* **2008**, *155*, 305.
16. Pan, B.; Xing, B. S. *J. Agr. Food Chem.* **2010**, *58*, 8338.
17. Yap, P. S.; Lim, T. T.; Lim, M.; Srinivasan, M. *Catal. Today* **2010**, *151*, 8.
18. Beck, J. S.; Vartuli, J. C.; Roth, W. J.; Leonowicz, M. E.; Kresge, C. T.; Schmitt, K. D.; Chu, C. T. W.; Olson, D. H.; Sheppard, E. W.; McCullen, S. B.; Higgins, J. B.; Schlenker, J. L. *J. Am. Chem. Soc.* **1992**, *114*, 10834.
19. Landskron, K.; Ozin, G. A. *Science* **2004**, *306*, 1529.
20. Zhang, F. Q.; Gu, D.; Yu, T.; Zhang, F.; Xie, S. H.; Zhang, L. J.; Deng, Y. H.; Wan, Y.; Tu, B.; Zhao, D. Y. *J. Am. Chem. Soc.* **2007**, *129*, 7746.
21. Ma, C. Y.; Mu, Z.; Li, J. J.; Jin, Y. G.; Cheng, J.; Lu, G. Q.; Hao, Z. P.; Qiao, S. Z. *J. Am. Chem. Soc.* **2010**, *132*, 2608.
22. Galarneau, A.; Cangiotti, M.; Renzo, F.; Fajula, F.; Ottaviani, M. F. *J. Phys. Chem. B* **2006**, *110*, 4058.
23. Machida, M.; Kikuchi, Y.; Aikawa, M.; Tatsumoto, H. *Colloid Surf. A-Physicochem. Eng. Asp.* **2004**, *240*, 179.
24. Ho, Y. S.; McKay, G. *Process Biochem.* **1999**, *34*, 451.
25. Langmuir, I. *J. Am. Chem. Soc.* **1918**, *40*, 1361.